 SDHM, vol.6, no.3, pp.161-188, 2010

Experimental and Numerical Investigation of 3D Mixed-Mode Crack Problems in Structures

H.A. Richard[1], M. Fulland[2], G. Kullmer[1] and N.-H. Schirmeisen[1]

Abstract: Fracture processes in real structures are in many cases of a three dimensional (3D) character. In this paper some basic problems of 3D-fracture processes are considered and discussed, in particular for general mixed-mode loading conditions, when modes I and II and III are superimposed. For experimental investigations an AFM-specimen is under consideration, while numerical simulations are carried out with the program ADAPCRACK3D.

Keywords: General mixed-mode Fracture, All Fracture Modes (AFM) Specimen, Computational 3D Crack growth simulations

1 Introduction

Fracture processes in real structures are in many cases of a three dimensional (3D) character. Due to general service loads an existing crack may experience complex loading conditions, which can be interpreted as a superposition of the three fundamental fracture modes I, II and III. The prediction of the developing 3D fracture process, which may be stable or unstable, is not yet well understood. There is a lack of physical understanding of those processes and furthermore qualified hypotheses are still missing for the prediction of the onset and the direction of crack growth and to assess critical crack dimensions. In particular there is a shortage of experimental findings regarding general 3D and mixed-mode fracture to form a solid basis on which the desired understanding and the missing fracture criteria could be established. This paper will contribute to this subject by reporting on the optimisation of the AFM-specimen with respect to advanced fracture and fatigue investigations for general 3D mixed-mode loading conditions. Findings of those experiments are capitalized for numerical three-dimensional crack growth analyses. The program ADAPCRACK3D is able to carry out such finite element simulations in real 3D structures.

[1] Institute of Applied Mechanics, University of Paderborn, 33098 Paderborn, Germany
[2] Hochschule ZiHau/Görlitz, 02763 Zittau, Germany

The field of 3D crack growth problems under mixed-mode loading conditions was under consideration by Prof. Dr. Fritz Buchholz for many years throughout his scientific career. In memoriam of his outstanding work in this field this contribution deals with this topic. Consequently important parts of this article rely on work elaborated by Prof. Buchholz. Additionally it is shown, in which way his contributions are incorporated into the newest development of 3D mixed-mode simulations.

2 The Mixed-Mode I–II–III–Problem

In the past 2D-problems of crack growth under mixed-mode I and II loading conditions have attracted much attention and through many investigations the problem is now well understood. A number of fracture criteria for predicting the onset of fracture and the direction of crack growth under mixed-mode I and II crack tip loading conditions are well established [Erdogan, F., Sih, G. C. (1963); Williams, J. G., Ewing, P. D. (1972); Sih, G. C., (1974); Hussain, M. A., Pu, S. I., Underwood, J. H., (1974); Nuismer, R. J., (1975); Wu, C. H., (1978); Palaniswamy, K., Knauss, W. G., (1978); Cotterell, B., Rice, J.R., (1980); Sumi, Y., Nemat-Nasser, S., Keer, L. M. (1983); Amestoy, M., Bui, H. D., Dang-Van, K., (1981); Richard, H.A., (1985); Leblond, J. B., Amestoy, M., (1989)]. In particular the CTS-specimen and the related special loading device, which have been designed by Richard [Richard, H.A., Hahn, H., G., (1980); Richard, H.A., (1981); Richard, H.A., Benitz, K., (1983)], and detailed theoretical, experimental and computational investigations have contributed to the current state in the field [Richard, H.A., Benitz, K., (1983); Banks-Sills, L., Arcan, M., Bui, H. D., (1983)].

In 2D or plane mixed-mode cases the basic relations can be presented in form of a fracture limit curve in a $K_I - K_{II}$ diagram (Fig. 1a). Unstable fracture will occur when the loading conditions at the crack tip, characterised by the stress intensity factors (SIFs) K_I and K_{II} reach any point on the 2D fracture limit curve [Richard, H.A., (1985, 1984)] (Fig. 1a). For mixed-mode fracture the extended crack will kink off from its initial direction (Fig. 2b) and for isotropic materials the kink angle is a function of the K_{II}/K_I ratio only[Richard, H.A., (1985)] (Fig. 2a). Besides other criteria[1−12] the $K_I - K_{II}$ fracture limit curve can be described by the following relation[Richard, H.A., (1985)]

$$K_V = \frac{K_I}{2} + \frac{1}{2}\sqrt{K_I^2 + 4\left(\alpha_1 K_{II}\right)^2} \leq K_{IC}. \tag{1}$$

In Eq. (1) K_V is the equivalent SIF and the parameter α_1 is the ratio K_{IC}/K_{IIC} of the related fracture toughness values. For some materials the values of α_1 are given in Tab. 1 according to[Richard, H.A., (1985, 1988)].

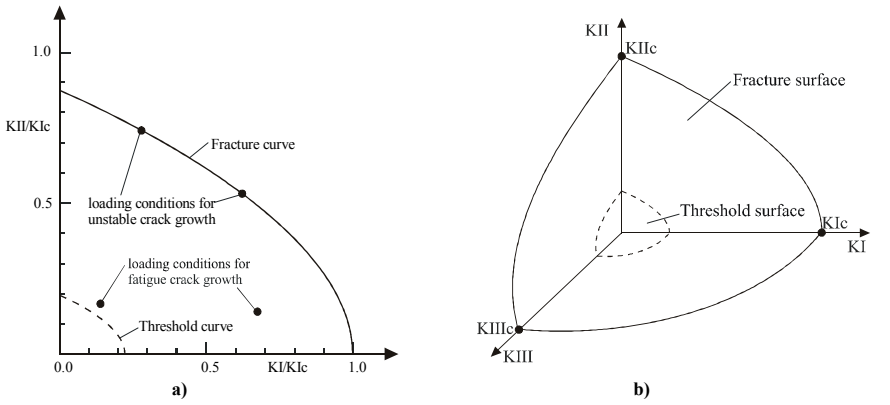

Figure 1: Threshold and fracture limit curves and limit surfaces a) for 2D or plane mixed-mode problems b) for 3D or general mixed-mode problems

The well established maximum tangential stress criterion [Erdogan, F., Sih, G. C. (1963)] and the maximum energy release rate criterion due to Nuismer[Nuismer, R. J., (1975)] can be well approximated with α_1=1.15 according to[Richard, H.A., (1985)]. The related kink angle can be predicted by the following relation

$$\varphi_0 = \pm \left[155,5^\circ \frac{|K_{II}|}{|K_I| + |K_{II}|} - 83,4^\circ \left[\frac{|K_{II}|}{|K_I| + |K_{II}|} \right]^2 \right] \tag{2}$$

in which $\varphi_0 < 0$ has to be considered for $K_{II} > 0$. A comparison of Eq. (2) with experimental findings[Richard, H.A., (1984); Richard, H.,A., Schöllmann, M., (1999)] is given in Fig. 2b.

Table 1: Values of α_1 for Different Materials

Material	α_1
PMMA	1,08
AlCuMg1	1,05
PVC, transparent	0,93
Steel, low alloy	1,28

For plane mixed-mode cases fatigue crack growth or stable crack growth can only develop if the crack tip loading conditions are characterised by a point lying between the fracture threshold and the fracture limit curve (Fig. 1a). In that case the

equivalent cyclic SIF

$$\Delta K_V = \frac{\Delta K_I}{2} + \frac{1}{2}\sqrt{\Delta K_I^2 + 6\Delta K_{II}^2} \tag{3}$$

is characterising crack growth[Richard, H. A., Linning, W., Henn, K., (1991)], which means da/dN is a function of ΔK_V. While for plane mixed-mode cases and isotropic materials fatigue crack growth is now well understood and can be predicted with good confidence and accuracy[Richard, H.,A., Schöllmann, M., (1999); Richard, H. A., Linning, W., Henn, K., (1991); Richard, H.A., May, B., Schoellmann, M., (1988); Hellen, T. K., Blackburn, W. S., (1975); Aoki,.S., Kishimoto, K., Yoshida, T., Sakata, M., Richard, H., A., (1990); Theilig, H., Doering, R., Buchholz, F.-G., (1997); Theilig, H., Buchholz, F.-G., (1999)], for the more general 3D mixed-mode problems only a few approaches are known[Kassir, M., K., Sih, G.,C., (1975)] and there is still a lack of understanding.

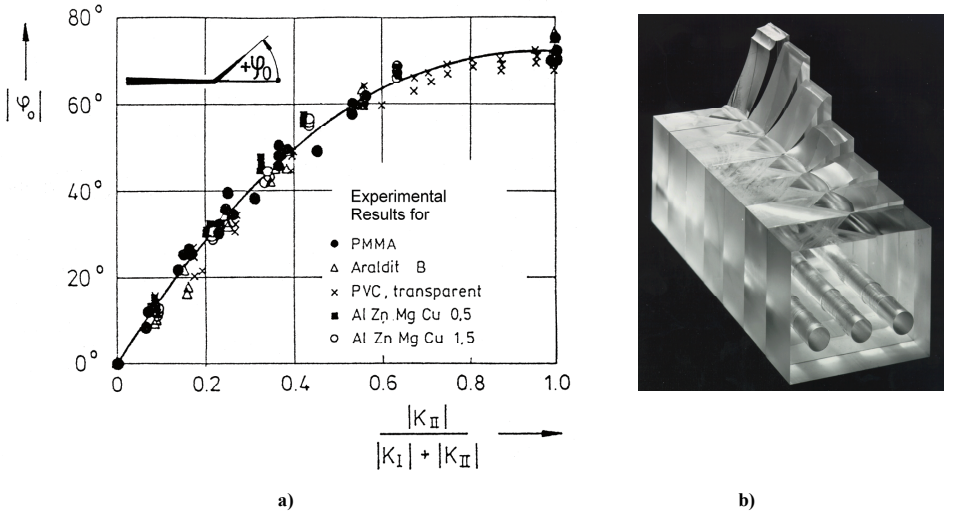

Figure 2: Crack kink angles φ_0, experimentally obtained by the aid of the CTS-specimen fractured under varying mixed-mode I + II loading conditions a) for specimens from different materials and predicted crack angles according to Eq. (2) b) for specimens from PMMA

Indeed in some more recent papers [Davenport, J. C. W., Smith, D. J., (1993); Pook, L. P., (1993, 1995); Hull, D. (1995)] investigations regarding superimposed

modes I and III are to be found, but these results can not be applied to cases of mode II and III and can not readily be generalised to cases where all basic fracture modes I, II, and III are involved. This situation can be explained best by the aid of Fig.1b. Unstable crack growth will develop, if a local loading condition along the crack front reaches a point on the fracture limit surface, which expands between the fracture limit curves for mode I and II, mode II and III and for mode III and I. Fatigue crack growth or stable crack growth develops if points characterising the local crack front loading conditions are lying between the threshold and the fracture limit surfaces. If along a crack front fatigue crack growth initiates under mixed-mode loading conditions a three dimensional curved crack surface begins to develop in the solid or specimen, as shown in Fig. 5a. The fracture limit surface can be represented by the following relation[Richard, H. A., (1983); Richard, H. A., Kuna, M., (1990)]

$$\left(\frac{K_I}{K_{IC}}\right)^u + \left(\frac{K_{II}}{K_{IIC}}\right)^v + \left(\frac{K_{III}}{K_{IIIC}}\right)^w = 1 \tag{4}$$

With u=1 and v=w=2 and $\alpha_1 = K_{IC}/K_{IIC}$ and $\alpha_2 = K_{IC}/K_{IIIC}$ by Eq. (4) a fracture criterion can be established

$$K_V = \frac{K_I}{2} + \frac{1}{2}\sqrt{K_I^2 + 4\left(\alpha_1 K_{II}\right)^2 + 4\left(\alpha_2 K_{III}\right)^2} \leq K_{IC}, \tag{5}$$

which covers also the most general cases where all fundamental fracture modes are superimposed. Whereas for plane mixed-mode problems the fracture limit curve is well established, with α_1=1.155, corresponding to the maximum tangential stress criterion, the value to be taken for α_2 has not yet been fixed. Furthermore the prediction of the local crack kinking, which is variable along the crack front, and the subsequent curvature of the three dimensional crack surface in space is widely open. Also the minimum strain energy density criterion [Kassir, M., K., Sih, G.,C., (1975)], which is considered to cover the most general cases with all modes superimposed, has to be proved experimentally in more detail. This is also holding for more recent 3D fatigue crack growth simulations [Mi, Y., Aliabadi, M. H., (1994); Wawrzynek, P. A., Carter, B. J., Potyondy, D. O., Ingraffea, A. R., (1994); Kuhn, G., Partheymüller, P., (1999); Dhondt, G., (1998); Schöllmann, M., Fulland, M., Richard, H.A., (2000a,b)].

In order to improve the situation further experimental and theoretical investigations have to be performed. A specimen with which all basic fracture modes I, II and III and all combinations of them can be investigated has been proposed by Richard [Richard, H.A., Hahn, H., G., (1982); Richard, H. A., (1983); Richard, H. A., Kuna, M., (1990)]. Namely this is the all fracture modes (AFM) specimen and the related special loading device, which briefly will be presented in the following

chapter, but for further details reference is given to Richard and Kuna [Richard, H. A., Kuna, M., (1990)]. Furthermore a detailed computational 3D fracture analysis of the AFM-specimen will be presented, which forms the basis of an improved and optimised design.

3 All Fracture Modes (AFM) Specimen

For experimental investigations of crack growth and fracture under different mixed-mode loading conditions several types of specimens are available[Erdogan, F., Sih, G. C. (1963); Richard, H.A., (1985, 1981); Richard, H.A., Benitz, K., (1983); Davenport, J. C. W., Smith, D. J., (1993); Pook, L. P., (1993)]. But none of these specimens covers the full range of all basic fracture modes or all combinations thereof. These requirements are fulfilled so far only by the AFM-specimen in combination with the special loading device (Fig. 3), which has been developed in particular for this purpose[Richard, H.A., Hahn, H., G., (1982); Richard, H. A., Kuna, M., (1990)].

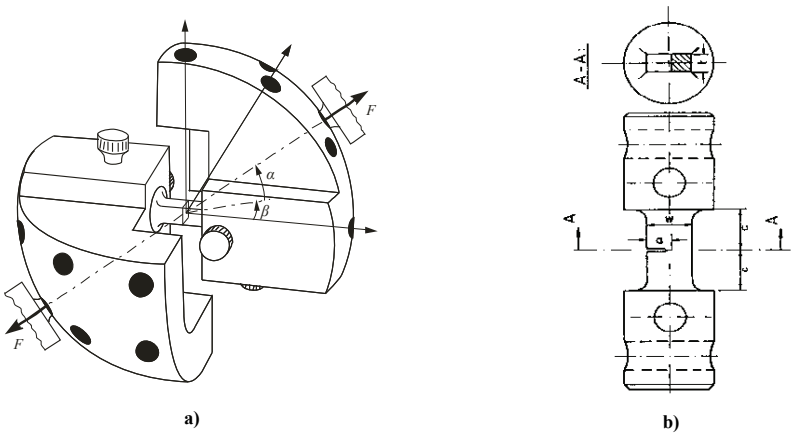

Figure 3: AFM-specimen and loading device a) loading device with loading angles α and β b) AFM-specimen with w=27mm, c=20mm, t=0.225w, a=0.5w

The design of this assembly is such that it can be mounted and loaded in a standard tensile/compression testing machine and that through the orientation of the loading device, with respect to the loading direction, the angles α and β of the applied tensile force F can be varied in order to generate any combination of superimposed fracture modes in the specimen. Furthermore the load line intersects the centre of the specimen at the front of the initial mode I fatigue crack or at the notch that

is machined there. So when the load F is acting under the angles α and β with respect to the local crack or notch tip coordinate system the components of F can be expressed as

$$F_y = N = F\cos\alpha\cos\beta \tag{6a}$$

$$F_x = Q = F\sin\alpha \tag{6b}$$

$$F_z = T = F\cos\alpha\sin\beta \tag{6c}$$

$$M_Q = Fc\sin\alpha \tag{6d}$$

$$M_T = Fc\cos\alpha\sin\beta \tag{6e}$$

and they are illustrated in Fig. 4a. The normal and shearing forces N and Q, T, respectively, are acting upon the cross-section ABCD of the specimen. The correlated internal forces N,Q,T and internal moments M_Q, M_T are acting in the upper and lower cross-sections of the specimen as shown in Fig. 4b. The bending moments M_Q and M_T are to compensate for the moments of the shearing forces Q and T with respect to the origin of the crack tip coordinate system. These stress resultants have to be transmitted from the loading device through the bolts and the bore holes onto the centre part of the AFM-specimen, which can be considered as a single edge notched (SEN) type of specimen. For further details reference is given to Richard and Kuna[Richard, H. A., Kuna, M., (1990)] again.

Consequently the following mean stresses and normalised SIFs can be defined

$$\sigma_N = N/wt \tag{7a}$$

$$\tau_Q = Q/wt \tag{7b}$$

$$\tau_T = T/wt \tag{7c}$$

$$K_{In} = K_I/\sigma_N\sqrt{\pi a} \tag{8a}$$

$$K_{IIn} = K_{II}/\tau_Q\sqrt{\pi a} \tag{8b}$$

$$K_{IIIn} = K_{III}/\tau_T\sqrt{\pi a} \tag{8c}$$

in order to normalise the results of the computational analysis.

Some experimental findings achieved with AFM-specimens are shown in Fig. 5. In particular in Fig. 5a a smoothly curved 3D crack surface can be seen in the AFM-specimen made from PMMA, which has initiated from the notch under loading conditions with α=60° and β=60°. For loading conditions with α=30° and β=60° the crack surface developed more irregular in an AFM-specimen made from AlCuMgPb (Fig. 5b).

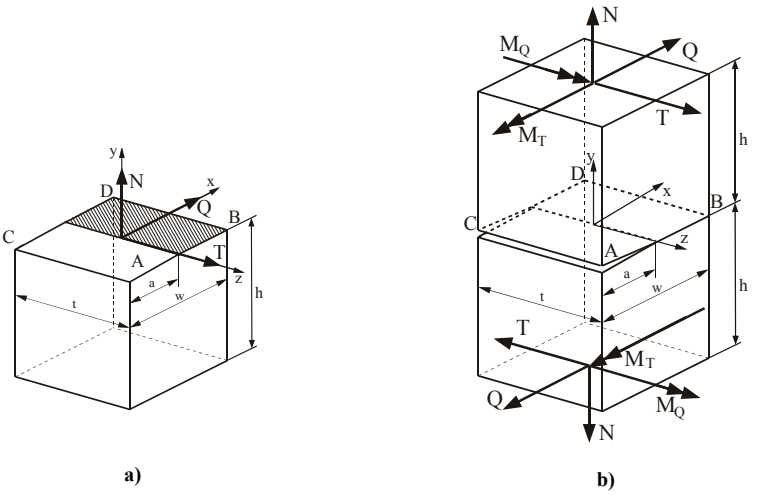

Figure 4: Stress resultants, generated in the AFM-specimen by a load F with load angles α and $\beta \neq 0$ a) acting upon the cracked cross-section b) acting upon upper and lower cross-sections

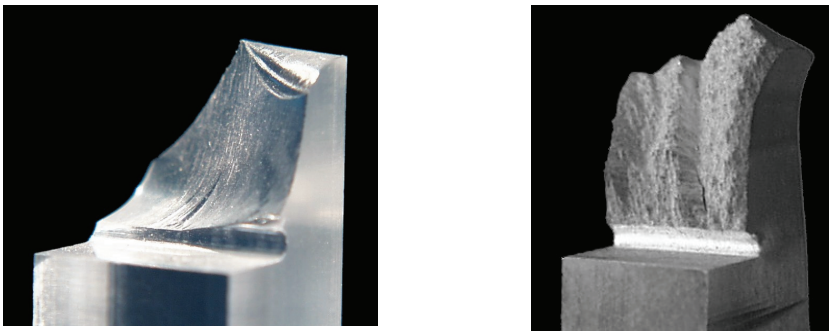

Figure 5: 3D curved crack surfaces in fractured AFM-specimens a) for PMMA and α=60˚, β=60˚ b) for AlCuMgPb and α=30˚, β=60˚

4 Virtual Crack Closure Integral (VCCI) Methods

4.1 VCCI or 2C-Method

For the fracture analysis of a mode I crack problem, Irwin's[Irwin, G. R., (1957, 1956)] well known analytical crack closure integral relation can be written in the

following FE-representation[Rybicki, E.F., Kanninen, M.F., (1977)]

$$G_I^{2C}\left(a+\frac{\Delta a}{2}\right) = \frac{1}{t\Delta a}W^y, W^y = \frac{1}{2}F_{y,i}(a)\cdot\Delta u_{y,j-1}(a+\Delta a) \tag{9}$$

which is holding for a FE-discretisation as given in Fig. 6a. By Eq. (9), in which t denotes the thickness of the specimen, the strain energy release rate (SERR) G_I is calculated on the basis of the work to be done by the nodal point force $F_{y,i}(a)$ against the relative nodal point displacement $\Delta u_{y,j-1}(a+\Delta a)$ in order to close the crack by Δa again (Fig. 6a). By Eq. (9) the numerical VCCI-method is defined for a 2D crack problem under mode I. It will be shown that through this method, which can be classified as a local energy approach, good results are obtained even for non-singular, low order standard elements and rather coarse FE-meshes, if the layout of the mesh around the crack tip is homogeneous.

The VCCI-method is also named and marked as 2C-method (2 calculations), because two FE analyses of the model have to be performed, respectively (for the crack lengths a and $a+\Delta a$), in order to compute one SERR result $G^{2C}(a+\Delta a/2)$ as mean value in the interval of finite crack extension Δa. But with respect to this effort it should be emphasised that by Eq. (9) the SERR is computed numerically exact for the actual FE discretisation under consideration, even for finite crack extensions Δa» 0. On that account no term lim$\Delta a \rightarrow 0$ is expressed in Eq. (9) and the notation $G^{2C}(a+\Delta a/2)$ stresses its meaning as the mean value of the SERR in the interval Δa of finite crack extension, which has to be correlated to $a+\Delta a/2$, the corresponding mean value of the crack length in the interval under consideration.

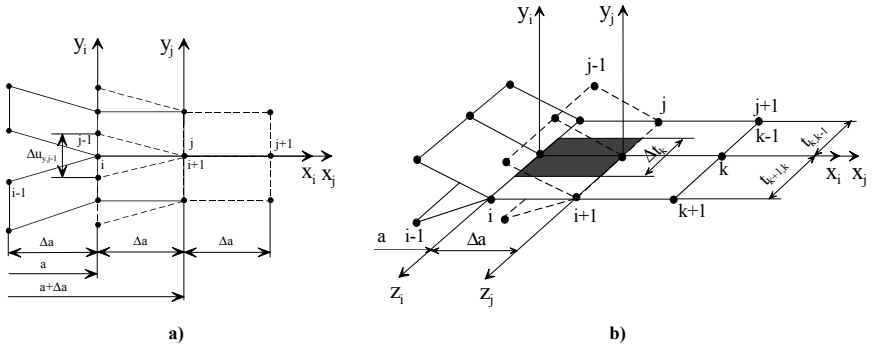

Figure 6: Computational VCCI-methods for 2D and 3D low order standard element discretisations a) 3- and 4-node membrane b) 6- and 8-node volume elements

4.2 MVCCI or 1C-Method

Rybicki and Kanninen[Rybicki, E.F., Kanninen, M.F., (1977)] have introduced the modified virtual crack closure integral (MVCCI) method in order to avoid the additional effort of a second FE-analysis for an extended crack of length $a+\Delta a$, respectively. This can be achieved if, with reference to Eq. (9) and to Fig. 6a, the required relative nodal point displacement $\Delta u_{y,j-1}(a+\Delta a)$ from the extended crack is replaced by the corresponding relative nodal point displacement $\Delta u_{y,i-1}(a)$ of the original crack with crack length a. By this numerically highly effective MVCCI or 1C-method (1 calculation) the SERR is calculated from

$$G_I^{1C}(a) = \lim_{\Delta a \to 0} \frac{1}{t\Delta a} W^y,\ W^y = \frac{1}{2} F_{y,i}(a)\,\Delta u_{y,i-1}(a). \tag{10}$$

The assumptions under which Eq. (10) is holding are the same as for Eq. (9). Through the term $\lim \Delta a \to 0$ in Eq. (10) it is expressed that the MVCCI or 1C-method is an approximate approach, with convergence to the exact solution only for $\Delta a \to 0$. But Rybicki and Kanninen[Rybicki, E.F., Kanninen, M.F., (1977)] have shown, that for small Δa also a good accuracy can be achieved by the MVCCI-method, with respect to reference solutions.

In the case of in-plane mixed-mode loading conditions at the crack tip or in the 3D-case including out-of-plane shear the additional mode II or mode III SERRs can be obtained readily by substituting the relevant x- and z-components of the nodal point forces and the relative nodal point displacements into Eq. (10). The total SERR at the crack tip or at a nodal point located along the crack front is then defined by

$$G_T^{2C}(a+\Delta a/2) = \sum_i G_i^{2C}(a+\Delta a/2), \quad i = I, II, III. \tag{11}$$

This numerically highly effective MVCCI-method for 2D-fracture analysis can be generalised in conjunction with standard low order volume element discretisations in a rather straight forward way in order to cover also complex 3D-fracture problems. Firstly Eqs. (9)-(11) have to be evaluated at all nodal point positions k =1, 2... along the crack front (Fig. 6b) and they have to be interpreted there with respect to a locally defined crack front coordinate system, respectively. Secondly the constant thickness t at the 2D-problems has to be replaced by an effective thickness Δt_k, which is correlated to the nodal point position k under consideration and evaluation (Fig. 6b). The resulting formulae are

$$G_I^{1C}(a,\Delta t_k)_k = \lim_{\Delta a \to 0} \frac{1}{\Delta t_k \Delta a} W_k^y, W_k^y = \frac{1}{2}\left(F_{y,i}(a)\,\Delta u_{y,i-1}(a)\right)_k, \tag{12a}$$

$$G_{II}^{2C}\left(a+\frac{\Delta a}{2},\Delta t_k\right)_k = \frac{1}{\Delta t_k \Delta a} W_k^x, W_k^x = \frac{1}{2}\left(F_{x,i}(a)\,\Delta u_{x,j-1}(a+\Delta a)\right)_k,, \tag{12b}$$

$$G_{III}^{2C}\left(a+\frac{\Delta a}{2},\Delta t_k\right)_k = \frac{1}{\Delta t_k \Delta a} W_k^z, W_k^z = \frac{1}{2}\left(F_{z,i}(a)\,\Delta u_{z,j-1}(a+\Delta a)\right)_k,, \tag{12c}$$

$$\Delta t_k = \frac{t_{k,k-1}+t_{k+1,k}}{2}, \tag{12d}$$

which are holding for 6- and 8-node volume element discretisations (Fig. 6b). In the following it will be shown that also in the 3D-case through this method, good results are obtained even for non-singular, low order standard elements and rather coarse FE meshes, if the layout of the mesh around the crack front is homogeneous.

Through Irwin's[Irwin, G. R., (1957, 1956)] analytical virtual crack closure relations the SERRs G_i are related to the SIFs K_i by

$$\begin{aligned} G_i &= \frac{K_i^2}{E'}, \quad i = I, II \\ E' &= \begin{cases} E & \text{for plane stress} \\ \frac{E}{1-\nu^2} & \text{for plane strain} \end{cases} \end{aligned} \tag{13}$$

and

$$G_{III} = (1+\nu)\frac{K_{III}^2}{E}. \tag{14}$$

The corresponding formulae for the VCCI-method for 3D crack problems can readily be developed from Eq. (9) and Eqs. (12a,b,c) respectively.

Through further generalisations of the method, also the numerically more effective non-singular, higher order elements can be utilised for the fracture analysis of 2D and 3D crack problems ([Buchholz, F.-G., (1984)]; [Krishnamurthy, T., Rammamurthy, T.S., Vijayakumar, K., Dattaguru, B., (1985)]; [Raju, I.S., (1987)]; [Sethuraman, R., Maiti, S.K., (1988)] and [Buchholz, F.-G., Schulte-Frankenfeld, N., Meiners, B., (1987); Buchholz, F.-G., Grebner, H., Dreyer, K.H., Krome, H., (1988)]; Narayana et al[Narayana, B., K., Krishnamurthy, T., Dattaguru, B., Ramamurthy, T.S., Vijay Kumar, K., (1988)]; [Shivakumar, K.N.: Tan, P.W., Newman, J.C.Jr., (1988)]; [Buchholz, F.-G., (1994); Ding, S., Buchholz, F.-G., Bürger, M., Kumosa, M., (1995); Buchholz, F.-G., Wang, H., Lin, J., Richard, H. A., (1998); Buchholz, F.-G., Chergui, A., Dhondt, G., (1999)]) and also other methods have been developed [Chan, S. K., Tuba, I. S., Wilson, W. K., (1970); Parks, D. M., (1974); Hellen, T. K., (1975); Kuna, M., (1982); Nikishkov, G.P., Atluri, S.N., (1987); Mi, Y., Aliabadi, M. H., (1995); Wawrzynek, P. A., Carter, B. J., Potyondy, D. O., Ingraffea, A. R., (1994); Dhondt, G., (1993, 1998); Kuna, M., Schmidt, V., (1984)].

5 Numerical Optimisation of AFM-Specimen

The 3D finite element analysis of the AFM-specimen in the original design was done by Richard and Kuna[Richard, H. A., Kuna, M., (1990)] by the aid of special hybrid singular crack tip elements[Kuna, M., (1982)] (HSE) and so these results are marked by „HSE“ in the following text and diagrams. Due to limited computer facilities the FE-model was restricted to the centre part of the AFM-specimen, and thus resulted in modelling a single edge notched (SEN) type of specimen, and furthermore the FE-model was rather coarse[Richard, H. A., Kuna, M., (1990)]. But the HSE-results given in Figs. (9-11) confirm that with this design of the AFM-specimen and the special loading device all general mixed mode I, II and III loading conditions at the crack front can be achieved with only one and the same specimen[Richard, H. A., Kuna, M., (1990)]. On the other hand, with respect to the objective to be able to generate pure and constant modes I or II or III loading conditions along the crack front, some disadvantages of the original design have been found. They will be discussed in conjunction with the findings presented in Figs. (9-11), in which the HSE-results according to Richard and Kuna[Richard, H. A., Kuna, M., (1990)] and the present MVCCI-results are compared.

But before this is done the computational accuracy of the 3D-fracture analysis by means of the MVCCI- method will be proved with respect to the correlated FE-model (Fig. 7) and concerning the non-singular, low order standard elements (6- or 8-node volume elements). This can be verified although for the 3D-case of the SEN-specimen no reference solution is available and furthermore for the SEN-specimen no 2D-reference solution is available [Tada, H. Paris, P., Irwin, G., (1973); Rooke, D. P., Cartwright, D. J., (1976); , (1987) (Ed.)] including the effect of finite length. This problem can be overcome by introducing symmetry conditions at the cracked side of the SEN-model, such that a centre cracked tension (CCT)-specimen is modelled for which finally a very detailed and well documented reference solution by Isida[Isida, M., (1973)] is available, including the finite length parameter c/w.

The way how to relate the results of the 3D-model of the CCT-specimen to the 2D-reference solution is to suppress all displacements in the thickness direction of the specimen (z-direction, see Fig. 4b) by setting $u_{z0}(x,y,z/t=\pm 0.5)=0$ as boundary conditions (BCs) at the front and rear surface of the specimen. By this trick plane strain conditions are enforced on the 3D-model of the CCT-specimen. In consequence these surfaces of the deformed specimen remain plane, even where the crack front intersects these surfaces, and so the SERRs evaluated along the crack front through the thickness of the specimen should be constant and related to the corresponding 2D reference value ([Isida, M., (1973)]).

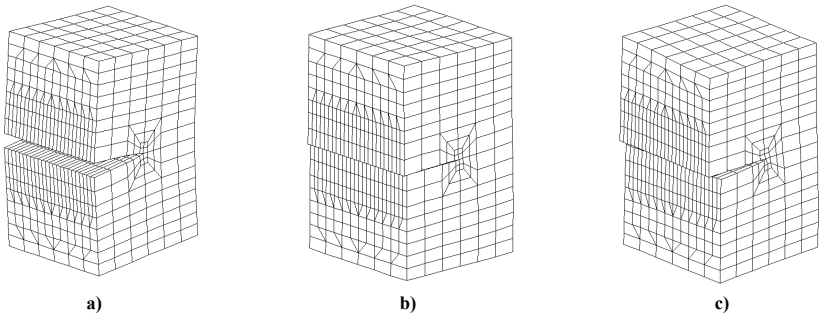

Figure 7: Deformed original AFM or SEN-models (a/w=0.5, t/w=0.9, c/w=0.75) a) under pure tension loading b) under pure in-plane shear loading c) under pure out-of-plane shear loading

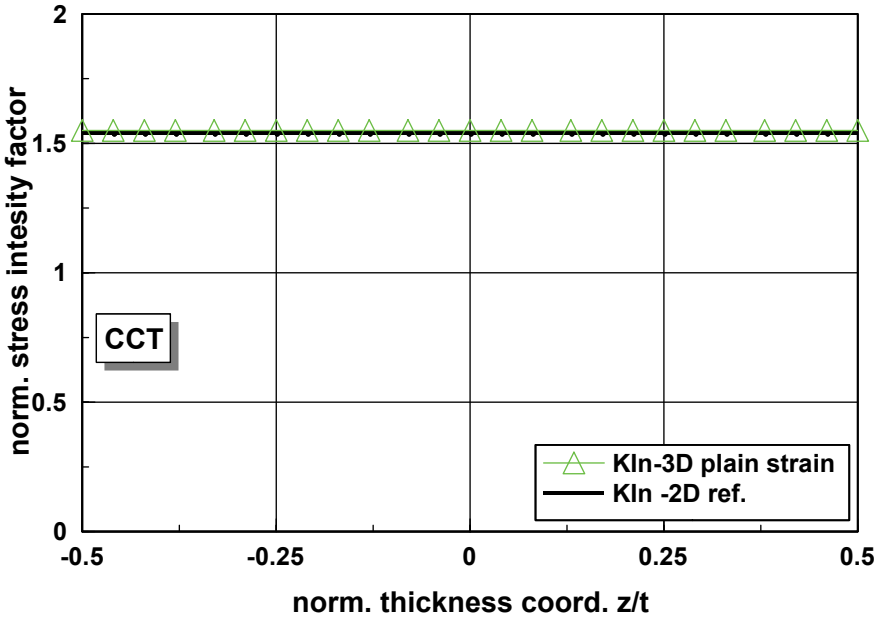

Figure 8: Norm. SIFs along the crack front of the 3D CCT-specimen with pl. strain BCs in thickness direction

In order to find a common basis for the comparison of the results the SERRs calculated by the MVCCI-method are converted into SIFs by the aid of Eq. (13) for i=I, II and by Eq. (14) for i=III. This finally results in the normalised SIFs as

plotted in Fig. 8. They are found to be perfectly constant along the crack front ($-0.5 \leq z/t \leq +0.5$) and through the minimal relative error of $\Delta rel = -0.19\%$, compared to the 2D plane strain reference value, this 3D FE-model of the CCT or SEN-specimen and the 3D generalisation of the MVCCI-method can be considered as highly qualified for the analysis of more general 3D fracture problems.

For the case of tension loading of the SEN-model (see Figs. 7a and 9) rather constant mode I loading conditions $K_{In}(a,z/t)$ are generated along the straight crack front through the thickness of the specimen ($-0.5 \leq z/t \leq +0.5$). Only adjacent to the locations where the crack front intersects the free surfaces of the specimen a slight drop of the normalised SIFs $K_{In}(z/t)$ are found with $z/t \rightarrow \pm 0.5$. This 3D-effect is well known from detailed 3D analyses of a CT-specimen and also the HSE and MVCCI-results for the SEN-model under tension loading confirm this effect by nearly coinciding results from both methods of analysis.

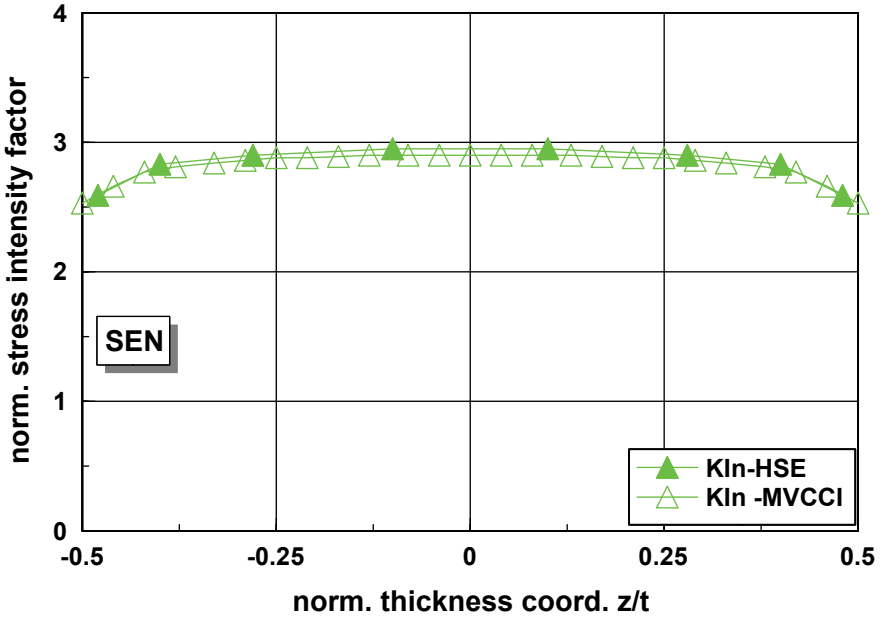

Figure 9: Norm. mode I - SIFs of the SEN-model under pure tension loading (a/w=0.5, t/w=0.9, c/w=0.75) HSE: FE-analysis with hybrid singular vol. elements[Richard, H. A., Kuna, M., (1990)] MVCCI: FE-analysis with 6- and 8-node vol. elements

The findings for pure in-plane shear loading of the SEN-model (Fig. 7b), as given in Fig. 10, are not so familiar any more. The mode II loading conditions along

the crack front through the thickness of the specimen are also found to be about constant, but here slightly increasing values for z/t$\rightarrow \pm 0.5$ are analysed. Consequently a 2D-analysis is no more be conservative as it still was the case for tension loading of the specimen (see Fig. 9). The HSE-results are not as smooth as the MVCCI-results, which may be due to the much coarser mesh of the related FE-model, in particular in the inner part of the specimen for -0.25$\leq$z/t$\leq$+0.25. But in addition to the intentionally generated mode II loading conditions K_{IIn}(a,z/t), also locally induced mode III loading conditions along the crack front are found by both methods of analysis. This mode coupling effect is related to Poisson's ratio and the laterally less constrained strains adjacent to the free surfaces of the specimen. Consequently in Fig. 10 K_{IIIn}(a,z/t) vanishes for the mid plane of the specimen (z/t=0) and shows increasing values of opposite sign for -0.4<z/t<0.4 and higher gradients for z/t$\rightarrow \pm 0.5$, where the crack front intersects the free surfaces of the specimen.

Because this mode coupling effect is related to Poisson's ratio of the material of the specimen it will generally be rather small and should not affect the local loading conditions considerably. That the discussed interpretation and understanding of this mode coupling effect is correct has been confirmed by a FE-analysis of this model with Poisson's ration ν set to zero (ν=0). In this case K_{IIn}(z/t) was found to be perfectly constant for -0.5$\leq$z/t$\leq$+0.5 and K_{IIIn}(z/t) was found to vanish completely for -0.5$\leq$z/t$\leq$+0.5. Finally it should be mentioned that although the mode III results of both methods generally agree very well, the HSE-results show a change in sign near to the mid-plane of the specimen. These values differ from the MVCCI-results but can not be confirmed on the basis of the relative nodal point displacements between the upper and lower crack surfaces.

For pure out-of plane shear loading of the SEN-model (Figs. 7c and 12) it turns out that the loading conditions achieved locally along the crack front are more difficult to understand. Firstly the findings given in Fig. 11 show an only approximately constant K_{IIIn}(a,z/t) distribution with a shallow maximum at z/t=0 and slightly decreasing values for z/t$\rightarrow \pm 0.5$. Here the HSE-results are about 7 % smaller, but with respect to the finer mesh of the corresponding MVCCI-model and the accuracy proved in the case of the CCT-model the presented MVCCI-results are considered to be more accurate.

But furthermore, in Fig. 11 remarkable mode II loading conditions along the crack front are analysed by both methods, although the specimen is subjected to pure out-of-plane shear loading. This means that here a distinct mode coupling effect is acting, by which through the intentionally generated mode III loading conditions along the crack front, also variable mode II loading conditions are included locally. Due to the level of the additionally induced mode II loading conditions one of the objectives to be achieved through the AFM-specimen is affected, namely, also to

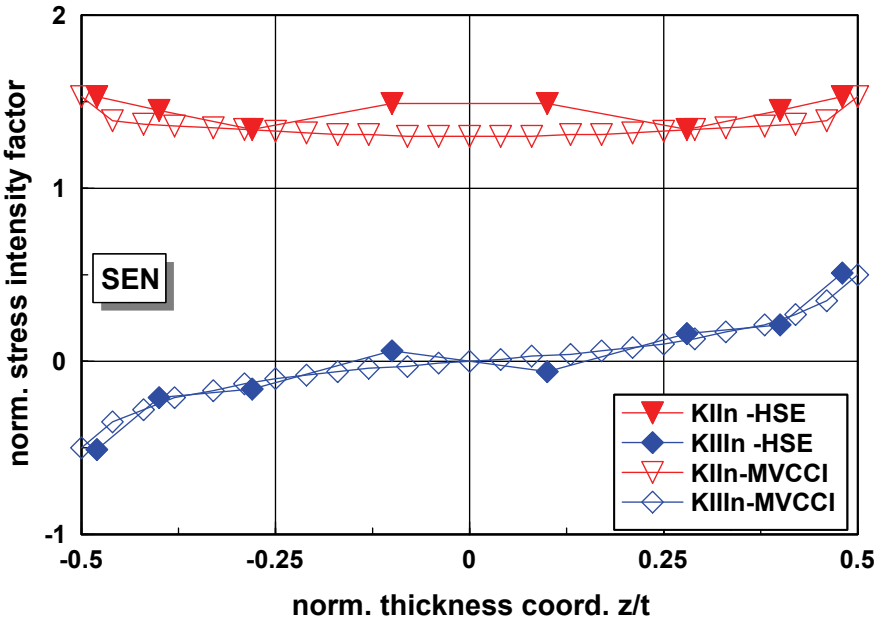

Figure 10: Norm. SIFs of the SEN-model under pure in-plane shear loading (a/w=0.5, t/w=0.9, c/w=0.75) HSE: FE-analysis with hybrid singular vol. elements[Richard, H. A., Kuna, M., (1990)] MVCCI: FE-analysis with 6- and 8-node vol. elements

be able to generate pure mode III loading conditions along the crack front. Although the induced K_{IIn}(z/t) values increase remarkably adjacent to the free surface their magnitudes indicate that they likely are not related to Poisson's ratio. This is confirmed by an analysis with ν set to zero again, for which in particular the K_{IIn}(z/t) distribution does not vanish along the crack front but remains mainly unaffected, apart from slightly smaller values for z/t$\rightarrow$0. In this case also the shape of the K_{IIIn}(z/t) distribution does not change to constant values versus z/t but remains mainly unaffected with only slightly smaller values, in particular for z/t$\rightarrow$0.

This strong coupling effect seems to be mainly due to the global deformation behaviour of the SEN-model under the applied out-of-plane shear loading, which is illustrated by the different views of the deformed SEN-model in Fig.12. In reference [Richard, H. A., Kuna, M., (1990)] it was found that for smaller values of the parameter t/w this coupling effect increases remarkably. This is confirmed by a detailed investigation by Chergui and Buchholz[Chergui, A., Buchholz, F.-G., (2000)] related to this problem, in which the geometrical parameters t/w and c/w of

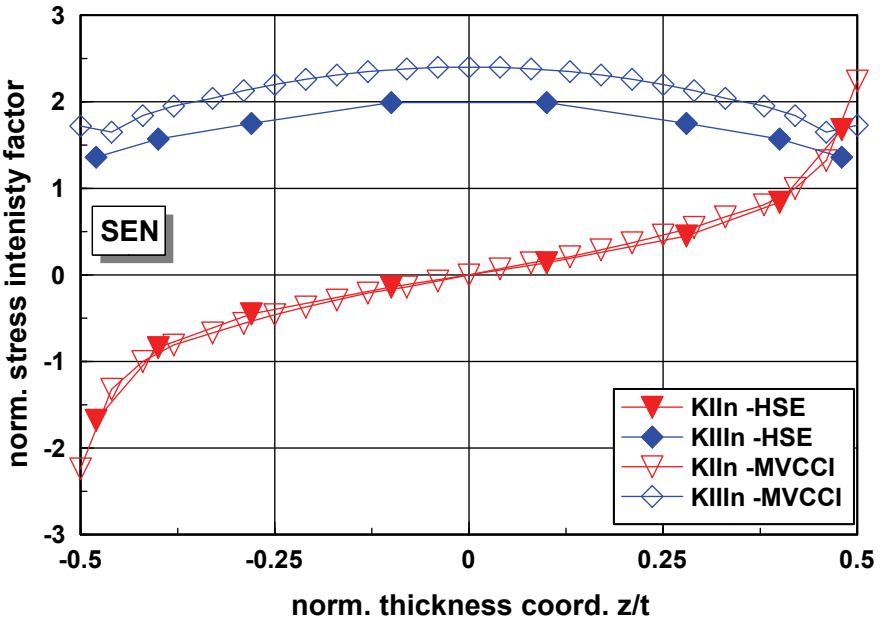

Figure 11: Norm. SIFs of the SEN-model under pure out-of-plane shear loading (a/w=0.5,t/w=0.9,c/w=0.75) HSE: FE-analysis with hybrid singular vol. elements[Richard, H. A., Kuna, M., (1990)] MVCCI: FE-analysis with 6- and 8-node vol. elements

the SEN-model have been varied systematically and in which it was shown that for smaller parameters c/w this pronounced coupling effect decreases considerably.

Further results concerning this AFM specimen are extensively discussed by Buchholz and Richard[Buchholz, F.-G., Richard, H. A., (2000)].

6 Imporvements of the AFM Loading Device

The described AFM specimen with the corresponding loading device allows for experiments with respect to the determination of the fracture surface. However, due to the relatively big mass of the standard loading device (comp. Fig. 3) fatigue experiments can only be done with very small testing frequencies. Therefore several improvements of the loading device were elaborated[Buchholz, F.-G., Richard, H.A., (2004)].

Fig. 13 shows an optimised version of the loading device with respect to weight reduction. In this design the additional mode III can be realised by rotating the

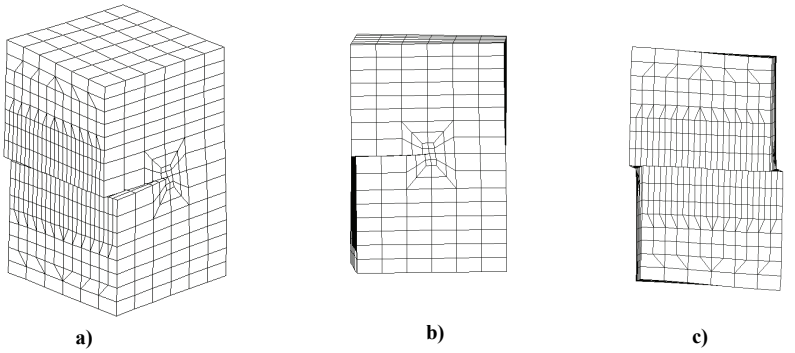

Figure 12: Deformed original AFM or SEN-models (a/w=0.5, t/w=0.9, c/w=0.75) under pure out-of-plane shear loading a) axonometric view b) front view c) side view

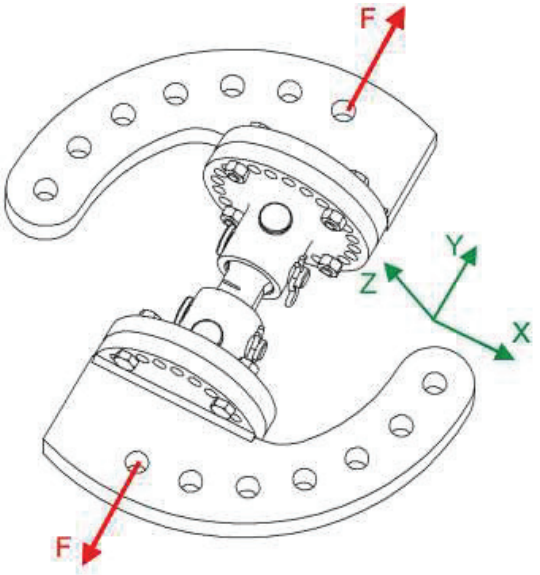

Figure 13: Improved design of the AFM loading device

specimen around the y-axis. Besides the smaller mass of the device also the handling in the assembling process in the testing machine is notably improved. The disadvantage of the design, however, is the relatively small stiffness of the device

in some loading positions which limits the materials that can reasonably be tested.

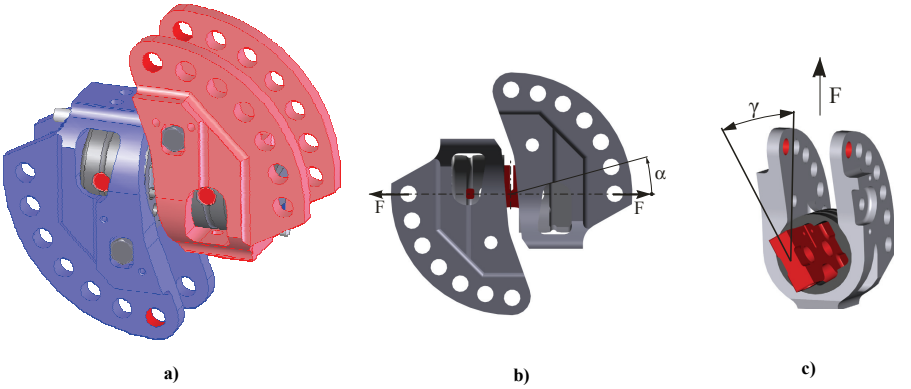

Figure 14: Latest version of the AFM loading device a) Fully assembled loading device b) Definition of the loading angle α c) Definition of the loading angle γ

Therefore recently a further improved design of the loading device (and the corresponding specimens) was developed (Fig. 14). As in the preliminary improved design (Fig.13) the outer part of the loading device allows for rotating the specimen about one axis (angle α) while the other angle γ is realised by a rotation of the specimen itself (Fig. 14c). This design allows for performing fatigue crack growth tests for the full range of mixed-mode I-II-III situations[Schirmeisen, N.-H.; Richard, H.A., (2009)]. First results gathered from those experiments are very promising (Fig.15).

7 Numerical Simulations of 3D Structures with Adapcrack3D

The results of the 3D mixed-mode experiments have been introduced into the 3D crack growth simulation code ADAPCRACK3D developed by the Institute of Applied Mechanics at the University of Paderborn. The basic functionality can be gathered from Fig. 16.

ADAPCRACK3D consists of three independent modules NETADAPT3D, ABAQUS^{TM} and NETCRACK3D. The results of the experiments with the AFM specimens were used for the development of the so called σ_1'-criterion[Schöllmann, M., Richard, H. A., Kullmer, G., Fulland, M., (2002)], which is a fundamental part or the fracture mechanical evaluations in the module NETCRACK3D. A detailed explanation of the functionality of ADAPCRACK3D can be found in literature[Schöllmann, M., Fulland, M., Richard, H.A., (2003); Fulland, M., Richard, H.A., (2005)].

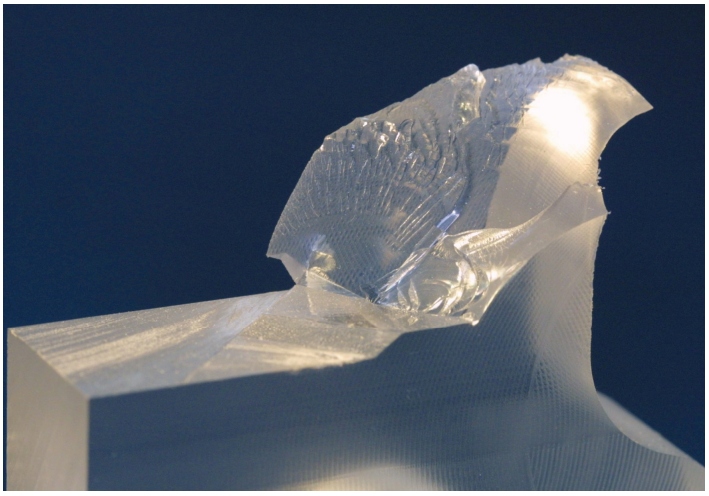

Figure 15: Example of a K_C-experiment for loading angles α=90° and γ=45°: Superimposed mode II and mode III loading

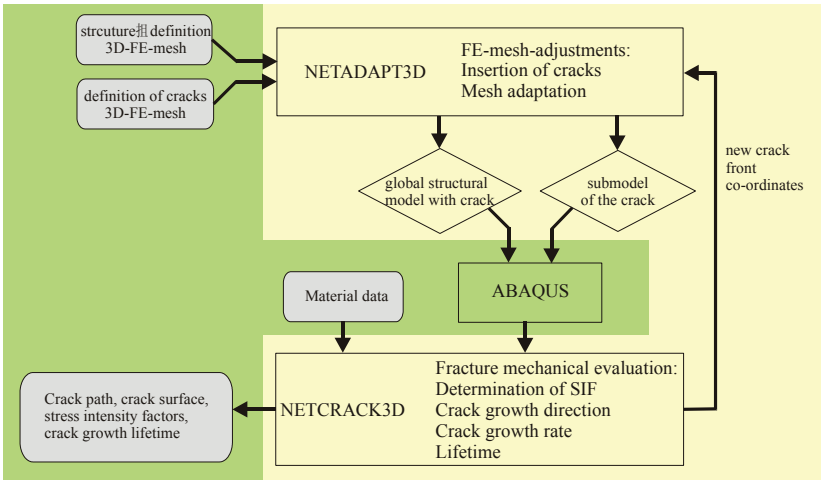

Figure 16: Simplified functionality scheme of the program ADAPCRACK3D

This program is able to carry out simulations of fatigue crack growth processes in arbitrary 3D structures[Fulland, M., Sander, M., Kullmer, G., Richard, H. A., (2008); Fulland, M., Sander, M., Richard, H. A., (2006)]. Figure 17 shows an example of a fatigue crack growth simulation in a flange shaft under torsional

loading. Throughout the simulation the developing crack fronts are subjected to varying mixed-mode loading situations. Besides the determination of the developing crack path ADAPCRACK3D is also able to calculate the lifetime of cracked structures even for cases of variable amplitude loading. Recent expansions of the program moreover cover the treatment of inhomogeneous and anisotropic material behavior[Fulland, M., Steigemann M., Richard, H.A., Specovius-Neugebauer, M., (2009, 2008)].

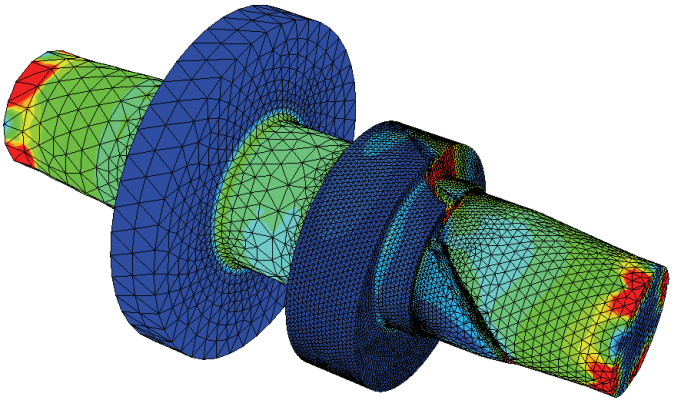

Figure 17: Crack growth simulation of a flange shaft under torsion

8 Conclusions

For general 3D fracture processes there still is a lack of understanding and furthermore a need to develop reliable and experimentally proved fracture criteria for the prediction of the initiation and the direction of crack growth. Based on the presented results a step may be done in this direction through further theoretical, experimental and computational investigations. Prof. Dr. Fritz Buchholz has played a major part in this development.

References

Amestoy, M., Bui, H. D., Dang-Van, K., (1981): Analytic asymtotic solution of the kinked crack problem. in: *Advances in Fracture Research*, ed. by Francois, D., 107-113.

Aoki,.S., Kishimoto, K., Yoshida, T., Sakata, M., Richard, H., A., (1990): Elastic-plastic fracture behavior of an aluminium alloy under mixed mode loading. *J. of Mechanics and Physics of Solids* 38, 195-213.

Banks-Sills, L., Arcan, M., Bui, H. D., (1983): Toward a Pure Shear Specimen for KIIC Determination, *Int. J. Fract*. 22, R9-R14.

Buchholz, F.-G., Richard, H. A., (2000): Optimisation of the AFM-specimen with respect to advanced fracture and fatigue investigations. In Meso-mechanical aspects of material behavior, Proceedings of the Special Symposium (Eds. K. Kishimoto, T. Nakamura, K. Amaya),Yufuin, Oita, Japan, 1-17.

Buchholz, F.-G., Richard, H.A., (2004): From Compact Tension Shear (CTS) to All Fracture modes (AFM) Specimen and Loading Devices, *Proc. of the Int. Conf. on Advances in Structural Integrity* (ICASI2004), Bangalore, India.

Buchholz, F.-G., (1984): Improved Formulae for the Finite Element Calculation of the Strain Energy Release Rate by the Modified Crack Closure Integral Method. In: *Accuracy, Reliability and Training in FEM Technology* (Ed. J. Robinson). Robinson and Associates, Dorset, 650-659.

Buchholz, F.-G., Wang, H., Lin, J., Richard, H. A., (1998): 3D finite element analysis of different test specimens for investigations on mixed mode I, II and III fracture. In: CD-ROM Proceedings of the 4th World Congress on Computational Mechanics (WCCM 98), Buenos Aires, Argentina.

Buchholz, F.-G., Schulte-Frankenfeld, N., Meiners, B., (1987): Fracture Analysis of Mixed-Mode Failure Processes in a 3D-Fibre/Matrix Composite Cylinder. In *Proc. 6th Int. Conf. on Composite Materials,* Vol. 3, (Ed. F.L. Matthews et al), Elsevier Appl. Science Publ., London, 3.417-3.428.

Buchholz, F.-G., Grebner, H., Dreyer, K.H., Krome, H., (1988): 2D- and 3D-Applications of the Improved and Generalized Modified Crack Closure Integral Method. In *Comp. Mech-anics 88,* Vol. 1 (Eds. S.N. Atluri et al.), Springer Verl., New York, 14.i.1-14.i.4.

Buchholz, F.-G., (1994): Finite Element Analysis of a 3D Mixed-Mode Fracture Problem by Virtual Crack Closure Integral Methods. In: *Fracture Mechanics* (Eds. A.V. Krishna Murthy, F.-G. Buchholz), Proc. of the Indo-German Workshop on Advances in Frature Mechanics, Indian Institute of Science, Bangalore, India, March 1994, Interline Publ., Bangalore, 7-12.

Buchholz, F.-G., Chergui, A., Dhondt, G., (1999): A comparison of SIF and SERR results with reference solutions regarding 3D and mode coupling effects for different specimens. In Fracture and Damage Mechanics 99 (Ed. M. H. Aliabadi), Dept.of Engng., Queen Mary and College, London.

Chan, S. K., Tuba, I. S., Wilson, W. K., (1970): On the finite element method in linear fracture mechanics. *Engng. Fracture Mech*. 2, 1-17.

Chergui, A., Buchholz, F.-G., (2000): 3D FE-Analysen zur bruchmechanischen Mode-Kopplung bei SEN-Proben unter nicht ebener Schubbelastung. *DVM-Bericht 232*, Deutscher Verband für Materialforschung und –prüfung, Berlin, 345-356.

Cotterell, B., Rice, J.R., (1980): Slightly curved or kinked cracks. *Int. J. Fract*. 16, 155-169.

Davenport, J. C. W., Smith, D. J., (1993): A study of superimposed fracture modes I, II and III on PMMA. Fat. Fract. *Engng. Mater. Struct.*, 16, 10, 1125-1133.

Dhondt, G., (1993): General behaviour of collapsed 8-node 2-D and 20-node 3-D isoparametric elements. *Int. J. Num. Meth. Engng*. 36, 1223-1243.

Dhondt, G., (1998): Cutting of 3-D finite element mesh for automatic mode I crack propagation calculation. *Int. J. Num. Meth. Engng*. 42, 749-772.

Dhondt, G., (1998): Automatc three-dimensional cyclic crack propagation predictions with finite elements at he design stage of an aircraft engine. Applied *Vehicle Technology Panel Symposium on Design Principles and Methods for Aircraft Turbine Engines (NATO-RTO)*, Toulouse, Frankreich.

Ding, S., Buchholz, F.-G., Bürger, M., Kumosa, M., (1995): 3D-Effects on Strain Energy Release Rates, Stresses and Stress Singularities Adjacent to Crack Front Edges. In: *Proc. of the Int. Conf. on Computational Engineering Science (ICES 95*), Mauna Lani, Hawaii, USA, August 1995 Springer Verlag, Berlin, 2039-2044.

Erdogan, F., Sih, G. C. (1963): On the crack extension in plates under plane loading and transverse shear. *Journal of Basic Engineering* 85, 519-527.

Fulland, M., Richard, H.A., (2005): Numerical three-dimensional crack growth simulation for components with multiple cracks.*CD-ROM Proceedings of the 11th International Conference on Fracture*, Torino, Italy.

Fulland, M., Sander, M., Kullmer, G., Richard, H. A., (2008): Analysis of fatigue crack propagation in the frame of a hydraulic press. *Engineering Fracture Mechanics* 75, 892-900.

Fulland, M., Sander, M., Richard, H. A., (2006): Three-dimensional crack growth simulation for a slat track, *CD-Rom Proceedings of LMS European User's Conference 2006*, Munich.

Fulland, M., Steigemann M., Richard, H.A., Specovius-Neugebauer, M., (2009): Automatic simulation of fatigue crack growth in three-dimensional structures consisting of functionally graded materials. *Proceedings of ICF12, 12th International Conference on Fracture*, Ottawa.

Fulland, M., Steigemann M., Richard, H.A., Specovius-Neugebauer, M., (2008): Numerical determination of fatigue crack growth in 3D structures consisting of non-homogeneous and/or non-isotropic material. *Proceedings of 17th European Conference on Fracture*, Brno.

Hellen, T. K., Blackburn, W. S., (1975): The calculation of stress intensity factors for combined tensile and shear loading. *Int. J. Fract*. 11, 605-617.

Hellen, T. K., (1975): On the method of virtual crack extension. Int. J. Num. Meth. Engng. 9, 187-208.

Hull, D. (1995): The effect of mixed mode I/III on crack evolution in the brittle solids. *Int. J. Fracture* 70, 59-79.

Hussain, M. A., Pu, S. I., Underwood, J. H., (1974): Strain energy release rate for a crack under combined mode I and mode II. In *Fracture Analysis,* ASTM STP 560. American Society for Testing and Materials, Philadelphia, 2-28.

Irwin, G. R., (1957): Analysis of stresses and strains near the end of a crack traversing a plate. *J. of Applied Mechanics* 24, 361-364.

Irwin, G. R., (1956): Onset of fast crack propagation in high strength steel and aluminium alloys. In *Sagamore Research Conference Proceedings*, Vol. 2, 289 - 305.

Isida, M., (1973): Analysis of Stress Intensity Factors for the Tension of the Centrally Cracked Strip with Stiffened Edges. *Engng. Fract. Mech*. 5, 647-665.

Kassir, M., K., Sih, G.,C., (1975): Three dimensional crack problems*, Mechanics of Fracture* 2, Noordhoff, Leyden.

Krishnamurthy, T., Rammamurthy, T.S., Vijayakumar, K., Dattaguru, B., (1985): Modified Crack Closure Integral Method for Higher Order Finite Elements. In *Finite Elements in Computational Mechanics* (Ed. T. Kant), Pergamon Press, Oxford, 891-900.

Kuna, M., (1982): Konstruktion und Anwendung hybrider Rißspitzenelemente für dreidimensionale bruchmechanische Aufgaben, Technische Mechanik 3, 37-43.

Kuna, M., Schmidt, V., (1984): An efficient finite-element-algorithm for three-dimensional fracture problem, In S. R. Valluri *(edt.), Advances in Fracture Research,* Proc. ICF6, New Delhi, Vol. 2. 1079-1086.

Kuhn, G., Partheymüller, P., (1999): 3D crack growth simulations with the boundary element method. In: B. Sarler, C.A. Brebbia, H. Power (eds.): *Moving Boundaries V* - Computational Modelling of Free and Moving Boundary Problems, WIT Press.

Leblond, J. B., Amestoy, M., (1989): The stress intensity factors at the tip of a kinked and curved crack. *Proc. 7th Int. Conf. Fract*. 3, 2339-234.

Mi, Y., Aliabadi, M. H., (1994): Three dimensional crack growth simulation using BEM. *Computers and Structures* 52, 871-878.

Mi, Y., Aliabadi, M. H., (1995): An automatic procedure for mixed-mode crack growth analysis. *Communications in Numerical Methods in Engineering* 11, 167-77.

Murakami, Y. (Ed.), (1987): *Stress Intensity Factors Handbook.* Pergamon Press, Oxford.

Narayana, B., K., Krishnamurthy, T., Dattaguru, B., Ramamurthy, T.S., Vijay Kumar, K., (1988): Modified Crack Closure Interal for Three Dimensional Crack Problems. Paper pres. at *Int. Conf. on Computational Engineering Science (ICES*), Atlanta, GA, USA.

Nikishkov, G.P., Atluri, S.N., (1987): Calculation of Fracture Mechanics Parameters for an Arbitrary Three-Dimensional Crack by the Equivalent Domain Integral Method. *Int. J. Num. Methods in Engineering* 24, 1801-1821.

Nuismer, R. J., (1975): An energy release rate criterion for mixed mode fracture. *Int. J. Fracture* 11, 245-250.

Palaniswamy, K., Knauss, W. G., (1978): On the problem of crack extension in brittle solids under general loading, *Mech. Today* (Ed. S. Nemat-Nasser), Vol. 4,. New York.

Parks, D. M., (1974): A stiffness derivative finite element technique for determination of elastic crack tip stress intensity factors. *Int. J. Fracture* 10, 487-502.

Pook, L. P., (1993): A finite element analysis of the angle crack specimen, *Mixed-Mode Fatigue and Fracture*, ESIS 14 (Edited by H. P. Rossmanith and K. J. Miller), Mechanical Engineering Publications, London, pp. 285-302

Pook, L. P., (1995): On fatigue crack paths, *Int. J. Fatigue* Vol. 17, No. 1, pp. 5-13.

Raju, I.S., (1987): Calculation of strain energy release rates with higher order and singular finite elements. *Engng. Fract. Mech.* 28, 251-274.

Richard, H.A., Hahn, H., G., (1980): Vorrichtung zur Ermittlung von ueberlagerter Normal- und Scherbeanspruchung in Proben. *Patentanmeldung,* Deutsches Patentamt, Muenchen.

Richard, H.A., (1981): An new compact shear specimen. *Int. J. Fracture* 17, R105-R107.

Richard, H.A., Benitz, K., (1983): A loading device for the creation of mixed mode in fracture mechanics. *Int. J. Fracture* 22, R55-R58.

Richard, H.A., (1984): Examination of brittle frature criteria for overlapping Mode I and Mode II loading applied to cracks. In G. C. Sih et al , *Application of Fracture Mechanics to Materials and Structures*. The Hague, 309-316.

Richard, H.A., (1985): Bruchvorhersagen bei überlagerter Normal- und Schubbeanspruchung von Rissen. *VDI-Forschungsheft 631*, VDI-Verlag, Düsseldorf.

Richard, H.A., (1988): Safety estimation for construction units with cracks under complex loading. *Int. J. of Materials* T*echnology* 8, 326-338.

Richard, H.,A., Schöllmann, M., (1999): Numerical investigation of fatigue crack growth under complex loading. In X.-R. Wu, Z.-G. Wang (Eds.), *Fatigue '99,* Vol. 2, Higher Education Press, Peking,, 839-844.

Richard, H. A., Linning, W., Henn, K., (1991): Fatigue Crack Propagation under Combined Loading, *Forensic Engineering*, Vol. 3, Nos. 2/3, 99-109.

Richard, H.A., May, B., Schoellmann, M., (1988): Prediction on fatigue crack growth under complex loading with the software system FRANC/FAM. In M. W. Brown et al (eds.), *Fracture from Defects,* Vol. II, EMAS Publ., West Midlands, 1071-1076.

Richard, H.A., Hahn, H., G., (1982): Verfahren und Vorrichtung zur von ueberlagerter Normal-, ebener- und nichtebener Schubbeanspruchung in Proben. *Patentanmeldung,* Deutsches Patentamt, Muenchen.

Richard, H. A., (1983): Praxisgerechte Simulation des Werkstoff- und Bruchverhaltens durch ueberlagerte Zug-, ebene Schub- und nichtebene Sxhubbelastung von Proben. *Jahrestagung 1983, Werkstoff- Bauteil- Schaden,* VDI-Gesellschaft Werkstofftechnik, Duesseldorf, 269-274.

Richard, H. A., Kuna, M., (1990): Theoretical and experimental study of superimposed fracture modes I, II and III, *Engng. Fracture Mech*.35, 949-960.

Rooke, D. P., Cartwright, D. J., (1976): *Compendium of stress intensity factors*. Her Majesty's Stationary Office, London.

Rybicki, E.F., Kanninen, M.F., (1977): A finite element calculation of stress intensity factors by a modified crack closure integral. *Engng. Fract. Mech.* 9, 931-938.

Shivakumar, K.N.: Tan, P.W., Newman, J.C.Jr., (1988): A Virtual Crack-Closure Technique for Calculating Stress Intensity Factors for Cracked Three Dimensional Bodies. *Int. J. of Fracture* 36, R43-R50.

Schirmeisen, N.-H.; Richard, H.A., (2009): Weiterentwicklung der AFM-Probe zur experimentellen Analyse räumlicher Mixed-Mode-Beanspruchung von Rissen.

DVM-Bericht 241, Deutscher Verband für Materialforschung und -prüfung e.V., Berlin, 211-220

Schöllmann, M., Richard, H. A., Kullmer, G., Fulland, M., (2002): A new criterion for the prediction of crack development in multiaxially loaded structures. *International Journal of Fracture* 117, 129-141.

Schöllmann, M., Fulland, M., Richard, H.A., (2003): Development of a new software for adaptive crack growth simulations in 3D structures. *Engineering Fracture Mechanics* 70, 221-230.

Schöllmann, M., Fulland, M., Richard, H.A., (2000a): Simulation of fatigue crack growth using the finite element method.,In *Proc. of the Int. Conf. on Computational Engineering Science (ICES 2000),* Los Angeles, USA (accepted for publication).

Schöllmann, M., Fulland, M., Richard, H.A., (2000b): 3-dimensional fatigue crack growth simulation under complex loading with ADAPCRACK3D. In *Proc. 13th Europ. Conf. on Fracture (ECF13),* San Sebastian, Spain (accepted for publication).

Sethuraman, R., Maiti, S.K., (1988): Finite element based computation of strain energy release rate by modified crack closure integral. *Engng. Fract. Mech*. 30, 227-231.

Sih, G. C., (1974): Strain energy density applied to mixed mode crack problems. *International Journal of Fracture*, 10, 305-321.

Sumi, Y., Nemat-Nasser, S., Keer, L. M. (1983): On crack branching and curving in a finite body. *Int. J. Fract*. 21, 67-79. Erratum in Int. J. Fract. 24, 159.

Tada, H. Paris, P., Irwin, G., (1973): *The stress analysis of cracks handbook*. Del Research Corporation, St. Luis.

Theilig, H., Doering, R., Buchholz, F.-G., (1997): A higher order fatigue crack path simulation by the MVCCI-method. In B. L. Karihaloo et al (eds), *Advances in Fracture Research*, Vol 4, Pergamon Press, Amsterdam, 2235-2242.

Theilig, H., Buchholz, F.-G., (1999): Crack path prediction by the MVCCI-method and experimental verification for specimens under proportional bending and shear loading. In C.Garcia Garino et al (eds), *Mecanica Computaciona* CD-ROM Proc. of MECOM 99, Asociacion Argentina de Mecnica Computacional, Santa Fe.

Wawrzynek, P. A., Carter, B. J., Potyondy, D. O., Ingraffea, A. R., (1994): A topological approach to modeling arbitrary crack propagation in 3D. In *Diana Computational Mechanics*, '94, ed. G. M. A. Kusters and M. A. N. Hendriks, Kluwer Academic, Dordrecht, 69-84.

Wawrzynek, P. A., Carter, B. J., Potyondy, D. O., Ingraffea, A. R., (1994): A topological approach to modeling arbitrary crack propagation in 3D. In *Diana Computational Mechanics'94* (Eds. G. M. A. Kusters and M. A. N. Hendriks), Kluwer Academic, Dordrecht, 69-84.

Williams, J. G., Ewing, P. D. (1972): Fracture under complex stress- the angle crack problem. *Int. J. Fract*. 8, 441-446.

Wu, C. H., (1978): Fracture under combined loads by maximum-energy-release-rate criterion, *J. Appl. Mech. ASME.* 45, 553-558.